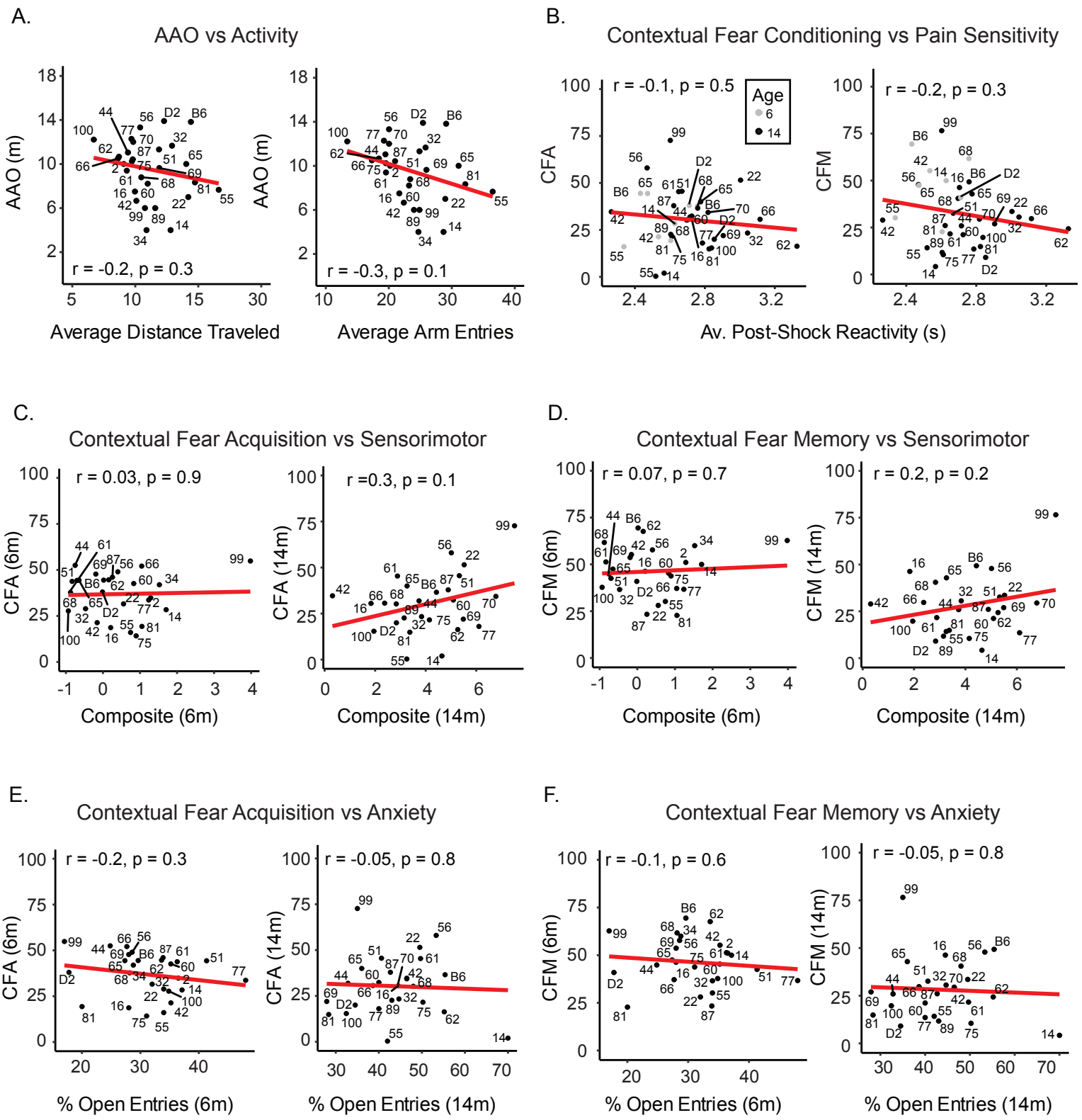
A.
AAO vs Activity
AAO (m)
r = -0.2, p = 0.3
Average Distance Traveled
r = -0.3, p = 0.1
Average Arm Entries
B.
Contextual Fear Conditioning vs Pain Sensitivity
CFA
r = -0.1, p = 0.5
Age
6
14
CFM
r = -0.2, p = 0.3
Av. Post-Shock Reactivity (s)
C.
Contextual Fear Acquisition vs Sensorimotor
CFA (6m)
r = 0.03, p = 0.9
Composite (6m)
CFA (14m)
r =0.3, p = 0.1
Composite (14m)
D.
Contextual Fear Memory vs Sensorimotor
CFM (6m)
r = 0.07, p = 0.7
Composite (6m)
CFM (14m)
r = 0.2, p = 0.2
Composite (14m)
E.
Contextual Fear Acquisition vs Anxiety
CFA (6m)
r = -0.2, p = 0.3
% Open Entries (6m)
CFA (14m)
r = -0.05, p = 0.8
% Open Entries (14m)
F.
Contextual Fear Memory vs Anxiety
CFM (6m)
r = -0.1, p = 0.6
% Open Entries (6m)
CFM (14m)
r = -0.05, p = 0.8
% Open Entries (14m)

Figure S1. Related to Figure 1: Cognitive traits are not directly associated with a variety of peripheral traits. A) Age at onset (AAO) of working memory deficits, as measured in the y-maze, is not correlated to (left) the average distance traveled or (right) average number of total arms entered. B) Neither (left) acquisition or (right) retention of contextual fear is significantly correlated to pain sensitivity as measured by post-shock reactivity. C) Contextual fear acquisition is not correlated to sensorimotor abilities at either (left) 6 months or (right) 14 months of age. D) Contextual fear memory (CFM) is not correlated to sensorimotor abilities at either (left) 6 months or (right) 14 months of age. E) Contextual fear acquisition is not correlated to anxiety, as measured by percent time spent in open arms on the elevated plus maze, at either (left) 6 months or (right) 14 months of age. F) Contextual fear memory (CFM) is not correlated to anxiety, as measured by percent time spent in open arms on the elevated plus maze, at either (left) 6 months or (right) 14 months of age.

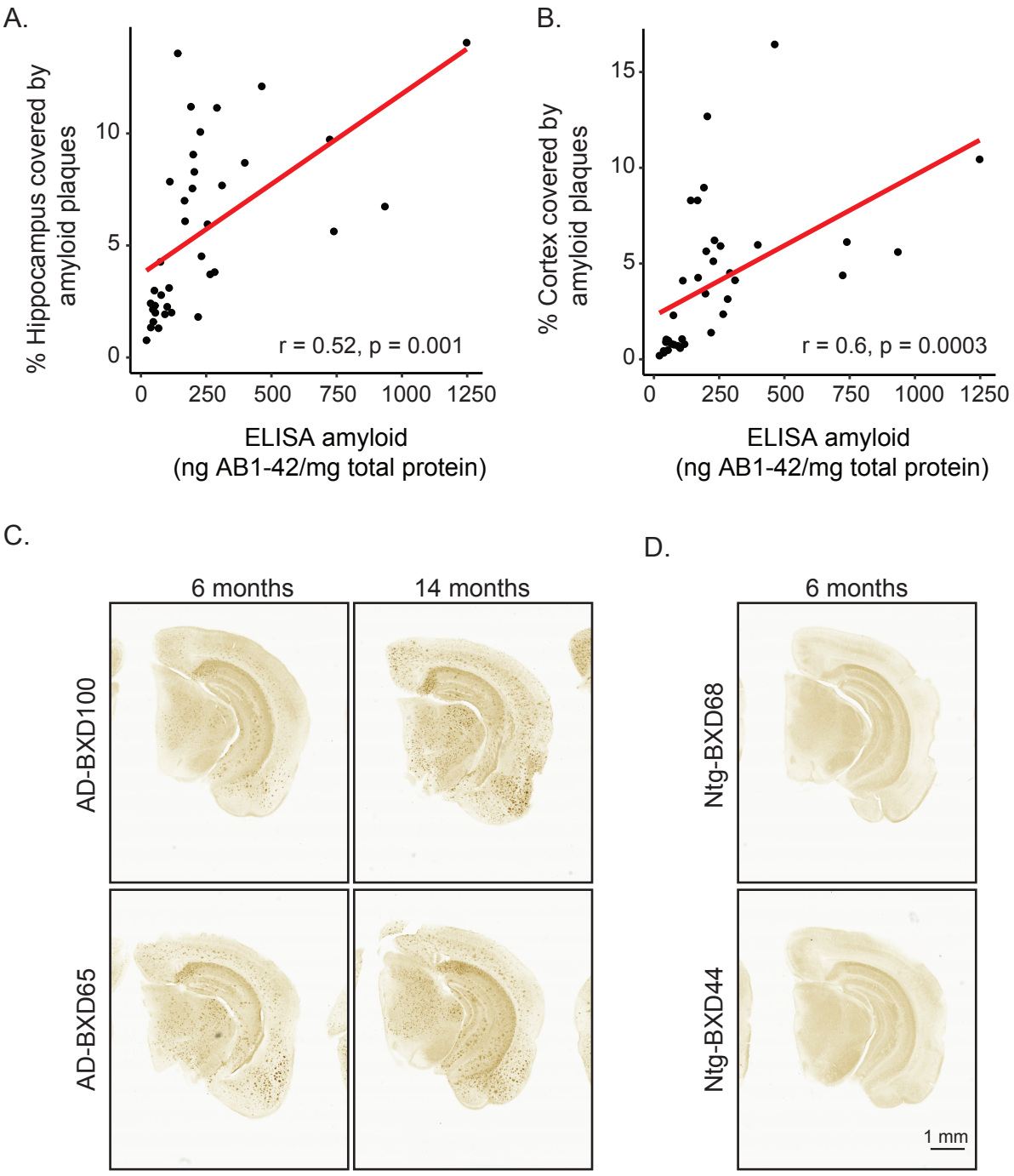

Figure S2. Related to Figure 1: AD-BXD mice develop plaques throughout the hippocampus and cortex. The percentage of A) the hippocampus and B) the cortex covered by amyloid plaques, as detected by Aβ1-42 immunohistochemistry and ImageJ particle analysis in a subset of AD-BXD mice, highly correlates with the overall levels of amyloid as detected by ELISA in a subset of mice where both assays were performed (n = 37). C) Representative images of plaque deposition in AD-BXD mice. D) No staining was detected in 6 month-old Ntg-BXD mice (n = 3). Scale bar = 1 mm.

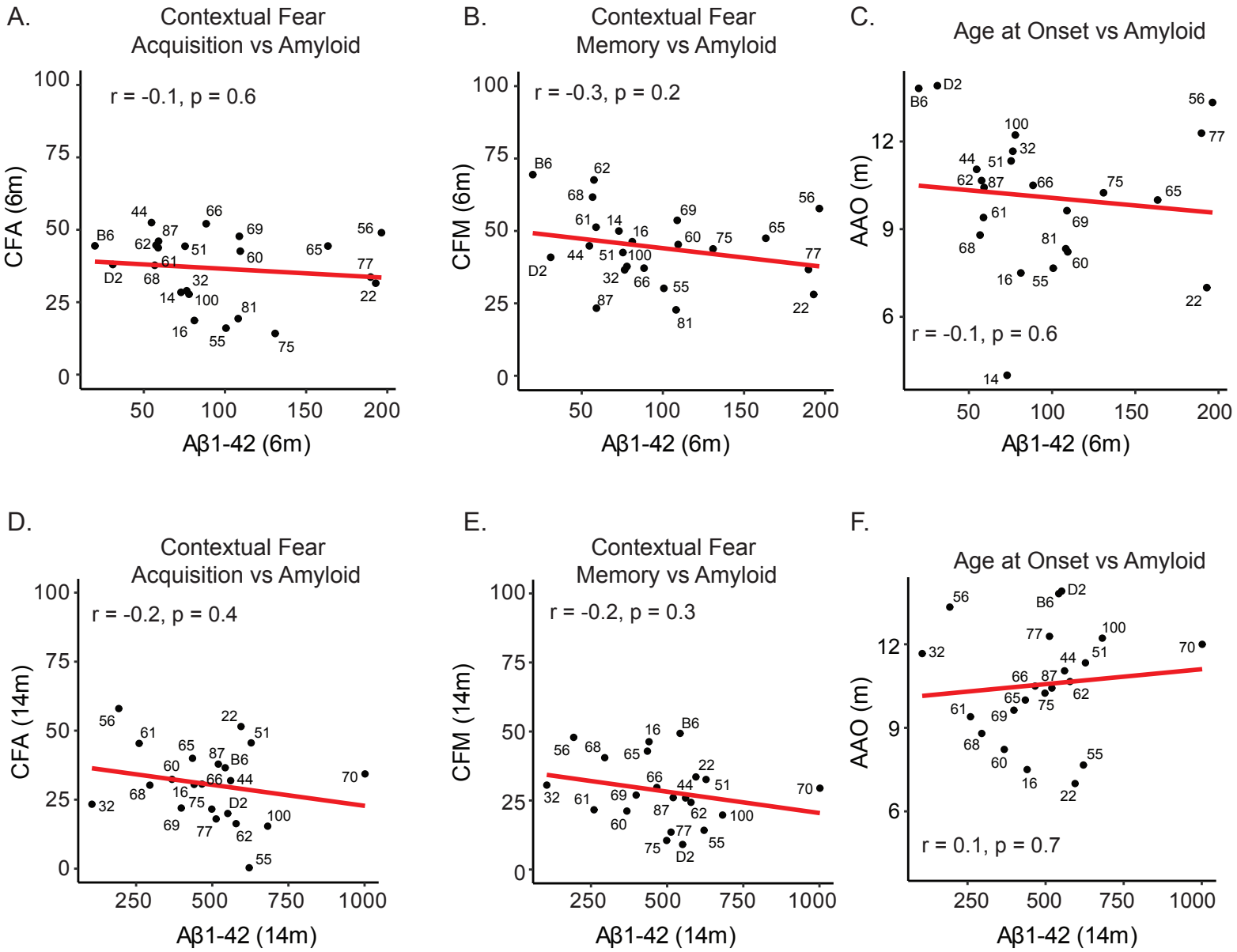

Figure S3. Related to Figure 1: Cognitive traits are not directly associated with amyloid levels. Amyloid levels, as measured by ELISA at 6m, are not significantly correlated to A) 6m contextual fear acquisition (CFA), B) 6m contextual fear memory (CFM), or C) age at onset (AAO) of working memory deficits. Amyloid levels, as measured by ELISA at 14m, are not significantly correlated with D) 14m CFA, E) 14m CFM, or F) AAO of working memory deficits.

A.

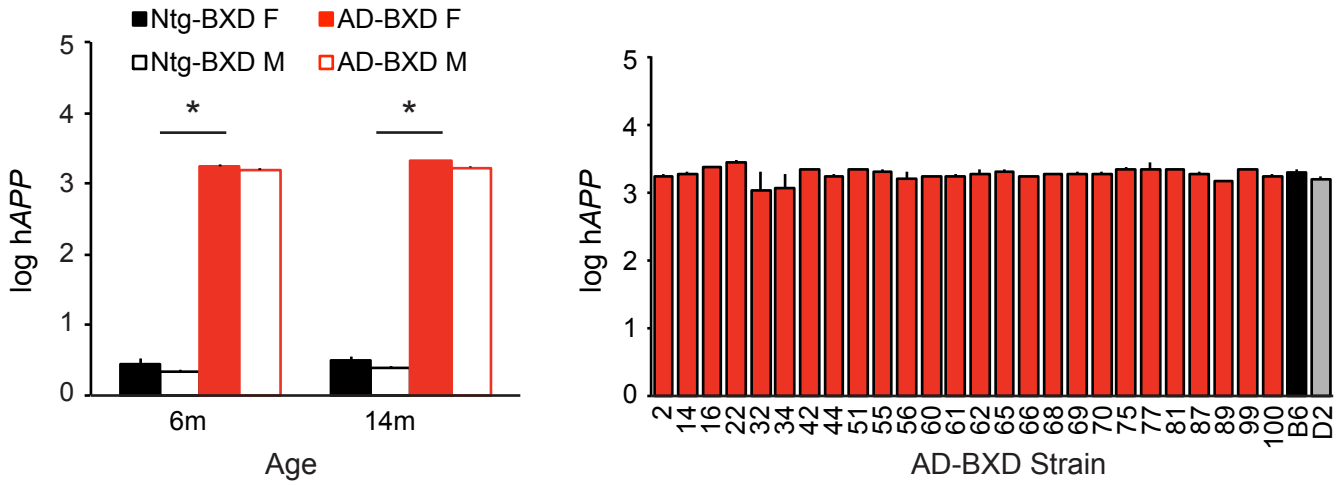
Human APP Expression
Ntg-BXD F
AD-BXD F
Ntg-BXD M
AD-BXD M
log hAPP
6m
14m
Age
AD-BXD Strain
2 14 16 22 32 34 42 44 51 55 56 60 61 62 65 66 68 69 70 75 77 81 87 89 99 100 B6 D2

B.

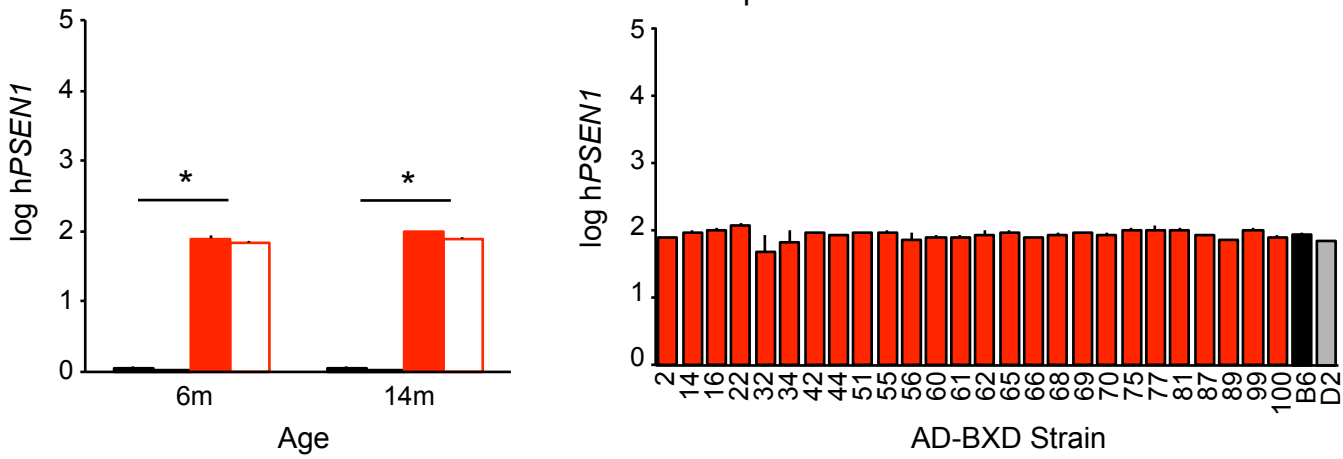
Human PSEN1 Expression
log hPSEN1
6m
14m
Age
AD-BXD Strain
2 14 16 22 32 34 42 44 51 55 56 60 61 62 65 66 68 69 70 75 77 81 87 89 99 100 B6 D2

C.

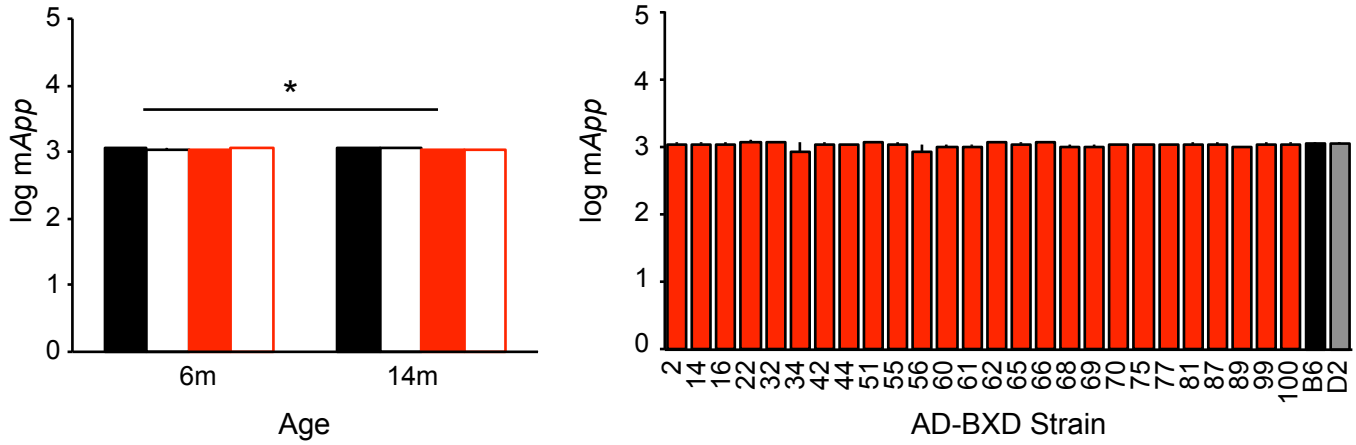
Mouse App Expression
log mApp
6m
14m
Age
AD-BXD Strain
2 14 16 22 32 34 42 44 51 55 56 60 61 62 65 66 68 69 70 75 77 81 87 89 99 100 B6 D2

D.

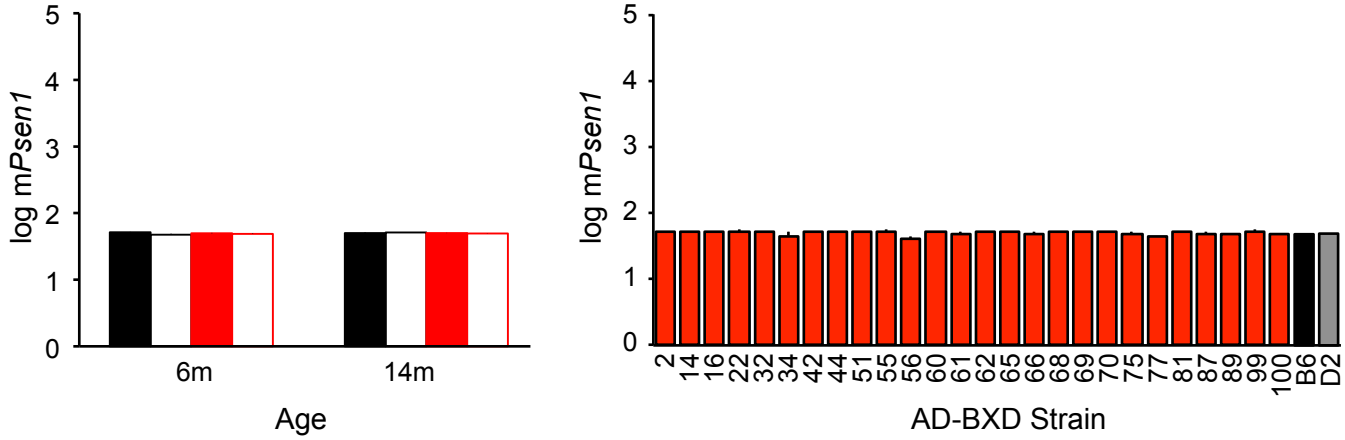
Mouse Psen1 Expression
log mPsen1
6m
14m
Age
AD-BXD Strain
2 14 16 22 32 34 42 44 51 55 56 60 61 62 65 66 68 69 70 75 77 81 87 89 99 100 B6 D2

Figure S4. Related to Figure 1: Background strain does not significantly modify 5XFAD transgene expression or endogenous App/Psen1 levels. Expression of mutated human *APP*/*PSEN1* and endogenous mouse *App*/*Psen1* evaluated in a larger subset of mice [n = 293 (177 females/116 males across 28 strains)]. (A, left) AD-BXD mice exhibited significantly greater h*APP* expression [$t(1, 291) = 92.3$, $p < 0.001$]. Across the AD-BXDs, there was no significant effects of age, sex, or (A, right) background strain. All 28 strains are shown here in comparison to only strains with Aβ42 data in Figure 1. (B, left) AD-BXD mice exhibited significantly greater h*PSEN1* expression [$t(1, 291) = 107.6$, $p < 0.001$]. Across the AD-BXD panel, there were no significant effects of age, sex, or (B, right) background strain on expression. (C, left) AD-BXD mice exhibit a slight but statistically significant decrease in m*App* expression relative to Ntg-BXDs [$t(1,291) = 2.6$, $p = 0.01$]. However, across the AD-BXD panel, there was no significant effect of age, sex, or (C, right) background strain on m*App* expression. (D, left) AD and Ntg-BXDs exhibit comparable endogenous *Psen1* expression. Across the population, there were no main effects of 5XFAD genotype, age, sex, or (D, right) AD-BXD background strain on m*Psen1* expression.

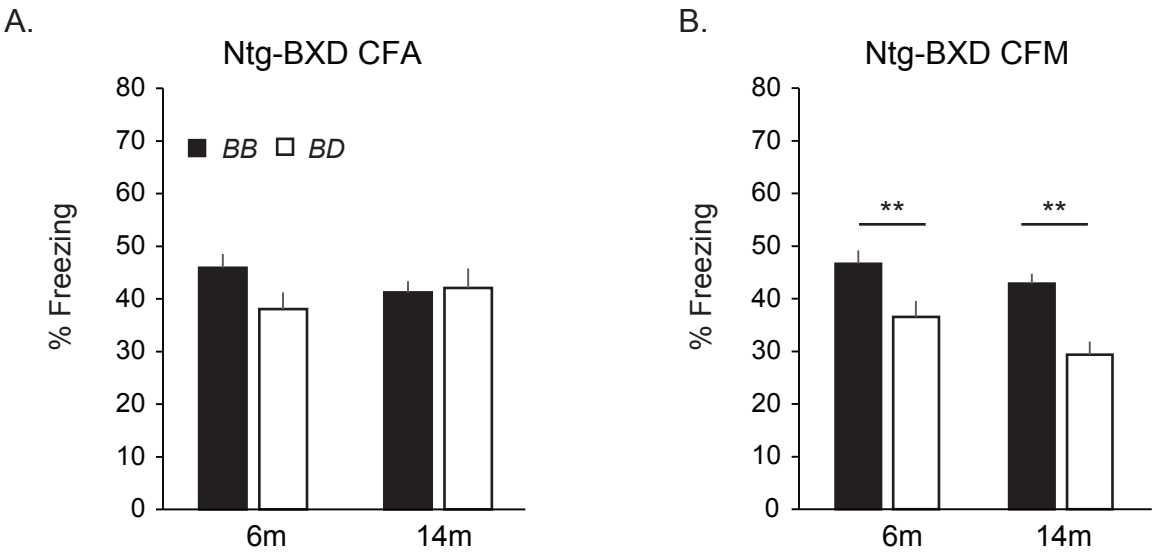

Figure S5. Related to Figure 2: Apoe genotype effects CFM, but not CFA, in Ntg-BXD mice. A) Across Ntg-BXD mice, there was no effect of Apoe genotype on CFA [$F(1, 280) = 0.3$, $p = 0.6$]. There were no additional effects of sex [$F(1,280) = 1.5$, $p = 0.2$], age [$F(1, 280) = 0.2$, $p = 0.7$], or interactions with Apoe genotype. B) Across Ntg-BXD mice, those carrying one copy of the D allele at Apoe performed significantly worse on CFM tests than mice with two copies of the B allele [$F(1, 280) = 12.0$, $p = 0.001$]. There were no additional effects of sex [$F(1, 280) = 0.3$, $p = 0.6$], age [$F(1, 280) = 2.3$, $p = 0.13$], or interactions with Apoe genotype.

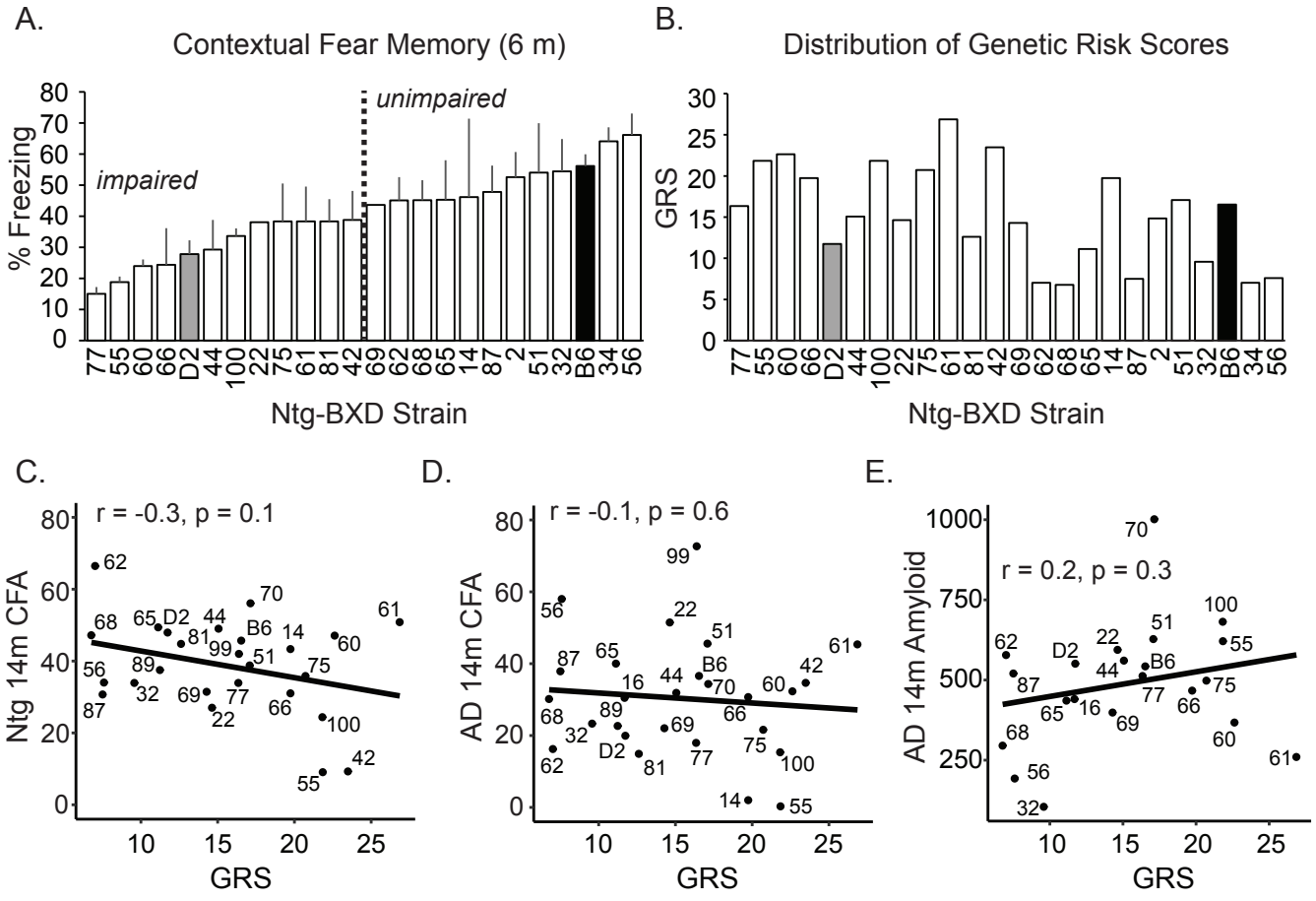

Figure S6. Related to Figure 3: AD genetic risk score defined in Ntg-BXD shows no relationship with cognitive outcomes. (A) Ntg-BXD strains were stratified into impaired (below population average) and unimpaired (above population average) based 6m CFM performance. (B) Genetic risk scores (GRS) were calculated for each strain based on allelic composition of 21 genes known to confer risk for AD, with the risk allele for each gene defined as that which appeared more frequently in the impaired population shown in (A). (C) GRS showed no relationship to 14m contextual fear acquisition (CFA) across Ntg-BXDs, (D) CFA in 14m AD-BXD mice, or (E) amyloid load at 14m in AD-BXDs.

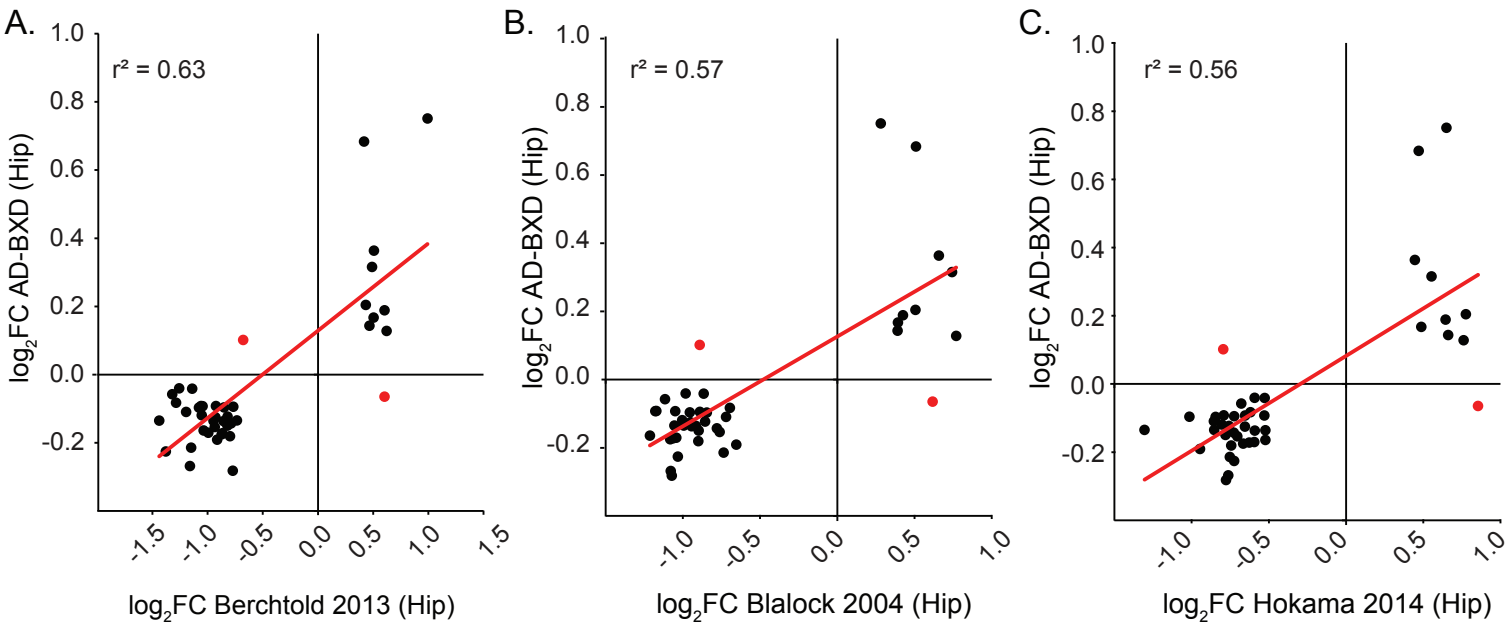

Figure S7. Related to Figure 5: AD-BXD panel exhibits high transcriptional concordance with human AD. Hargis and colleagues (Hargis and Blalock, 2016) recently identified a transcriptional signature of AD, consisting of the top 10% of upregulated and downregulated genes common to four different human AD datasets. To evaluate transcriptional concordance between our panel and human AD, the direction and magnitude of change was compared across mouse and human datasets. Specifically, the log2 fold change (FC) of gene expression between AD- and Ntg-BXDs is plotted on the y-axis, while the log2 fold change of gene expression between human AD patients and controls plotted on the x-axis. A) Log2FC of 39/60 (65%) AD signature genes is concordant between our mouse panel and a study by Blalock et. al., 2011 (Blalock et al., 2011). B) Log2FC of 39/59 (68%, one AD gene not detected in human dataset) AD signature genes is concordant between our mouse panel and a study by Blalock et al., 2004 (Blalock et al., 2004). C) Log2FC of 39/60 (65%) AD signature genes is concordant between mouse and human using dataset by Hokama et al., 2014 (Hokama et al., 2014). Secondary analyses of human datasets, see (Hargis and Blalock, 2016). Each point represents a gene; log2 fold changes with opposite directionality have been highlighted in red.

Supplementary Tables

Table S1. Related to Figure 4: Tab 1, list of genes differentially expressed between all AD-BXDs relative to all Ntg-BXDs. Tabs 2-3, Gene ontology (GO) terms significantly enriched among differentially expressed genes (adjusted p-value < 0.05), as identified by ranked gene set enrichment analysis (GSEA).*See spreadsheet

Table S2. Related to Figure 5: List of AD transcriptional signature genes identified by Hargis and Blalock (2017) as the top 10% commonly upregulated and downregulated genes across human AD datasets and their expression profile across mouse and human datasets.*See spreadsheet

Table S3. Related to Figure 5: List of genes differentially expressed in late-stage mouse AD (between 14m AD-BXDs and 14m Ntg-BXDs) and in mouse normal aging (between 6m Ntg-BXDs and 14m Ntg-BXDs) as identified by DESeq2.*See spreadsheet

Table S4. Related to Figure 5: List of GO terms significantly enriched among differentially expressed genes in mouse AD (Tab 1) or mouse normal aging (Tab 2). For comparison, we identified those pathways containing enough genes to be identified in each set (Tab 3) for use in graphing relative enrichment in mouse AD vs mouse normal aging.*See spreadsheet

Table S5. Related to Figure 1 and STAR Methods: Data used for comparing mutated human *APP* and *PSEN1* (i.e. 5XFAD transgene expression) and endogenous mouse *App* and *Psen1* across genetic backgrounds.